Applications of Heart Shaped Glass Spoon Loop Oscillating Heat Pipe (HSGS/LOHP) for Making Coffee Stirrer

Namphon Pipatpaiboon[1], Thanya Parametthanuwat[2], Nipon Bhuwakietkumjohn[2], Sampan Rittidech[3], Surachet Sichamnan[1*]

[1] Department of Mechanical Engineering, Faculty of Industry and Technology, Rajamangala University of Technology Isan, Sakon Nakhon Campus, Sakon Nakhon 47160, Thailand
[2] Heat Pipe and Nanofluid Technology Research Unit, Faculty of Industrial Technology and Management, King Mongkut's University of Technology North Bangkok, Bangkok 10800, Thailand
[3] Division of Mechanical Engineering, Faculty of Engineering, Mahasarakham University, Maha Sarakham 44150, Thailand

Corresponding Author Email: surachet.si@rmuti.ac.th

ABSTRACT

This study aimed to investigate the application of a Heart Shaped Glass Spoon Loop Oscillating Heat Pipe (HSGS/LOHP) made of a glass tube. The results showed that HSGS/LOHP can be practically used for stirring hot coffee in a cup. At the working substance filling rates of 80 and 60%, slug and annular flows of the working substance pattern were found while at 40% only the slug flow was found. The maximum mean lengths of the slug and annular flows of the working substance were 0.0259 and 0.00443 m which occurred at the working substance filling rate of 80% at the evaporator temperatures of 40°C, the average velocity was the highest for every working substance filling rate at the evaporator temperatures 70°C. The slug and annular flow patterns had maximum speeds of 0.00171 and 0.00111 m/s when tested at the 40% and 60% working substance filling rates, respectively. The working substance at the evaporator temperature of 40°C and the filling rate of 80% had the highest buoyancy force and moment of inertia of 4.90 ± 0.25 kN and 901.77 ± 45.08 Tm^2·kg, respectively.

1. INTRODUCTION

Upon considering heat transfer or heat exchange processes, Oscillating Heat Pipe (OHP) often attracts considerable attention. OHP is generally available in 3 forms, Close End Oscillating Heat Pipe (CEOHP), Close Loop Oscillating Heat Pipe (CLOHP), and Close Loop Oscillating Heat Pipe with Check Valve (CLOHP/CV) as shown in Figure 1.

All three types of OHPs consist of 3 parts: the evaporator section, the adiabatic section, and the condenser section. The tube is vacuumed and filled with the working substance which alternates between liquid slugs and vapor bubbles which is also known as slug trains. The working principle of OHP is based on the latent heat of vaporization of the working substance inside the pipe. When the OHP's evaporator is heated by a heat source, the working substance boils, transforms from a liquid slug to a vapor bubble and moves within the tube in an oscillating pattern. The vapor bubbles will move the heat from the evaporator section through the adiabatic section to the condenser section before releasing it through the pipe's surface to the heat sink. The vapor bubbles of the working substance then condense and flows along the tube's wall back to the evaporator section due to Earth's gravity. The continuous cycle is subsequently initiated repeatedly [1, 2]. Heat pipes are widely used due to their thermal efficiency of heat transfer, even at minimal temperature difference between the evaporator section and condenser section [3]. OHP usage and improvement of its thermal efficiency has received continuous development,

including the application of CLOHP/CV to increase the efficiency of air conditioning system. According to the tests, the cooling loads were increased by 3.6% after applying the highest values at 14.9% for COP and 17.6% for EER. The results of this study were anticipated to provide an approach to improving the efficiency of indoor air conditioning systems which helps to reduce energy waste [4]. When using CLOHP/CV in combination with a circular tube solar collector system, the CLOHP/CV could increase the system efficiency by 76%. Thus, it is ideal for winter applications [5]. The application of CLOHP/CV in drying process could reduce an average of 28.13% of energy consumption, when compared with the conventional hot air dryers [6]. For low temperature areas, using OHP with a solar collector system helps to increase the temperature of the hot water in the system. Furthermore, the inclination angle also affects thermal properties of a solar collector [7]. Oscillating heat pipe heat exchanger has also been used as a heat recovery device in an air conditioning system to enhance humidity reduction capacity of the evaporator coil. Using methanol, binary, and water as working substances, the efficiencies were enhanced by 25%, 21%, and 17%, respectively. By using the same working substances, the total energy savings were 1,932 W, 1,849 W and 1,645 W, respectively [8]. Additional applications such as using 0.5 wt% silver nanoparticles mixed with ethanol as working substance showed that the silver nanoparticles in ethanol produce a good contact angle, reducing wetting capacity, thereby, increasing thermal behavior [9]. To determine thermal efficiency of the

oscillating heat pipes (PHP), two active substances, ethanol and acetone, were mixed with ratios 6:1, 3:1, 1:1, 1:3 and 1:6 and filling ratios of 30%, 50% and 70. % by volume were used as working substances. The evaporator was heated by a 10–50 W power source while cooling at the condenser was done using cooled air. Results revealed that working substances were key factors for the thermal efficiency of PHP. Increasing acetone content in the active substance raised PHP's thermal dissipation. On the other hand, thermal resistance was decreased when input thermal power increased. The best efficiency was achieved by using; a 1:6 volumetric ratio of ethanol and acetone, a 50% filling ratio, and a 90° inclination angle [10]. In addition, more studies were conducted to improve the heat transfer rate of the heat pipes by using an external magnetic field to strengthen the heat transfer of the heat pipe. Results showed that, under the influence of various external magnetic fields, heat pipe with nano-magnetic fluid as a working substance provided a better heat transfer than the heat pipe which used water as a working substance. The best heat transfer rate could be achieved with the highest adjustment rate of 19.2% [11]. Further development including shape and structural modifications of OHP enhance greater applications ability. Such developments encompassed the study of two-phase flow patterns within the Helical Oscillating Heat Pipe [12]. This included the study of the effect of Internal Diameter and Working substances on Thermal Performance of a Vertical Closed-Loop Oscillating Heat Pipe with Double Heat Sources [13] and a study of the thermal characteristics of Three-Dimensional Coil Type Pulsating Heat Pipe at different heating modes [14].

OHP has been studied in previous research to; increase its thermal efficiency and use to variety of applications. However, OHP's application in household utensils received very little attention. Therefore, this research was conducted to ascertain the possibility of designing and producing a hot coffee stirrer that can be used in daily life, based on working principles of the Loop Oscillating Heat Pipe (LOHP). Such application combines the knowledge of heat pipes, heat transfer, dual-state flow, and product design. Results showed that the heart-shaped glass spoons with HSGS/LOHP can be practically used in daily life like a common coffee spoon. Main attraction of the heart-shaped spoon made from HSGS/LOHP is an observable dual-state flow pattern which moves through the condensation portion of a glass spoon. Such distinctive design symbolizes health-conscious perceptions of coffee drinkers who observe the dual-state flow pattern in the heart-shaped condensation part of the spoon. In addition, the findings can be commercialized to create products with higher market values.
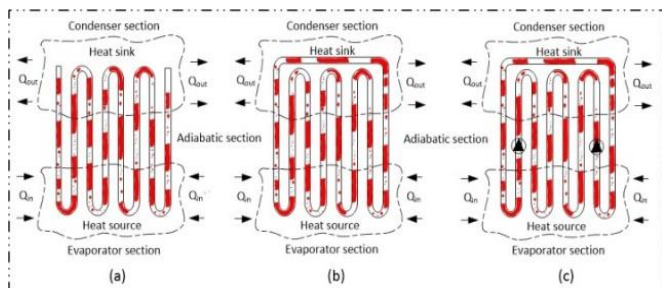

Figure 1. Three types of Oscillating Heat Pipes (OHPs) (a) CEOHP, (b) CLOHP, and (c) CLOHP/CV

2. THE EXPERIMENTAL APPARATUS AND ANALYSIS

2.1 Method

An important factor to consider when designing and building an HSGS/LOHP is the inner diameter of the pipe. HSGS/LOHP was designed and made, in reference to working principles of the Oscillating Heat Pipe (OHP), by using a small glass tube with an internal diameter (ID) of 3.4 mm and thickness (t) of 0.8 mm. The design resembled an actual coffee spoon. Further details of the spoon are shown in Figure 2 (A) and (B). OHP's inner diameter clearly distinguishes it from the conventional heat pipe as the oscillating working substance occurs along the axial direction of the pipe. Thus, the inner diameter of the pipe determines the occurrence of vapor and liquid mass [3]. For this research, the maximum inner diameter of HSGS/LOHP was determined from equation (1) [9, 15].

$$d_{i,\max} = 2\sqrt{\frac{\sigma}{\rho_l g}} \qquad (1)$$

where, $d_{i,max}$ is the maximum internal diameter of the capillary tube (m), σ is the surface tension of the working substance (N/m), ρ_l is the density of the working substance in its liquid state (kg/m^3), g is the acceleration due to gravity (m/s^2).
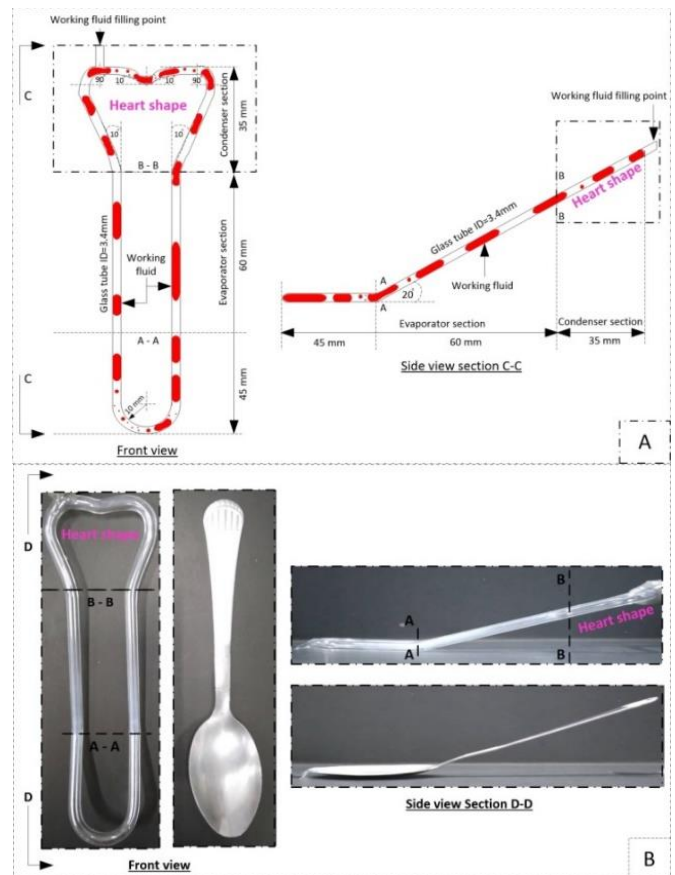

Figure 2. Details and design of a Heart Shaped Glass Spoon Loop Oscillating Heat Pipe (HSGS/LOHP)

2.2 The equipment, instrument setup and HSGS/LOHP

Figure 3 shows schematic diagram of the equipment and instrument setup. The controlled and variable parameters

shown in Table 1. The process began with constructing HSGS/LOHP made from a glass tube with the inner diameter of 3.4 mm which resembles the shape and size of a common teaspoon as per Figures 2(a) and 2 (b). The tube was vacuumed using a vacuum pump connected to the working substance filling as shown in Figure 3(a). After vacuuming, the HSGS/LOHP was filled with the working substance which alternated between Vapor Slug and Liquid Slug, which is also known as Slug train as illustrated in Figure 3(b). The instrument setup and test procedure are shown in Figure 3(c). HSGS/LOHP received hot coffee acted as the heat source for the HSGS/LOHP's evaporator. The parameter in this study consisted of temperature at the evaporator section (hot coffee in a cup) were 70, 60, 50, and 40°C, the working fluids were deionized water mixed with food coloring at a concentration of 1% by volume, the filling rates were 80, 60, and 40% of the evaporator section volume. The condenser section in this test was a natural cooling characteristic of the heart-shaped part. Test was done at the ambient temperature of 25°C and inclination angle used was 45° as show in Figure 3(c).

Table 1. Controlled and variable parameters

Conditions	Details
Independent variables	- Temperatures at the evaporator section (hot coffee in a cup) were 70, 60, 50, and 40°C - Working substance filling rates were 80, 60, and 40% of the evaporation volume (Fr).
Dependent variables	- Behaviors and flow pattern at the HSGS/LOHP' s condenser - Effect of filling ratio and evaporator's temperature on the flow pattern within the HSGS/LOHP's condenser section - Effects of evaporator section temperature on buoyancy and moment of inertia of the flow pattern within the condenser of HSGS/LOHP - Effects of the evaporator temperature on Reynolds Number (Re) and Heat Flux in the condenser section of HSGS/LOHP
Control variables	- The working substance used was deionized water mixed with food coloring at a concentration of 1% by volume. - Test was done at the ambient temperature of 25°C - Oscillating glass heat pipe for heart-shaped glass spoon had an internal diameter of 3.4 mm (Details as shown in Figure 2) - The inclination angle used was 45°

According to the experiments as show in Figure 3(c), the evaporator section of HSGS/LOHP was soaked in the hot coffee within a cup. The condenser section of HSGS/LOHP is cooled by natural cooling. Three temperature measurement points were set up to determine the temperature of the hot coffee within a cup, wall temperature of condenser section and ambient, temperatures at three points were also recorded using a K type thermocouples with ± 1.5°C that had the cable connected to a data logger (Yokogawa DX200) with ± 1 °C accuracy. The HSGS/LOHP condensation flow pattern was recorded with a video camera. The resulting video files were analyzed to characterize the flow patterns, the flow speeds, the length of the flow patterns, the buoyancy force, and the moment of inertia of each flow pattern at the condenser, the Reynolds Number (Re) and the heat flux. Results of the experiment were due to; the behaviors and flow patterns at the HSGS/LOHP's condenser, the effect of filling ratio and

evaporator's temperature on the flow pattern within the HSGS/LOHP's condenser, the effects of the evaporator section temperature on buoyancy force and moment of inertia of the flow pattern within the condenser of HSGS/LOHP, the effects of the evaporator temperature on Reynolds Number (Re) and Heat Flux in the condenser of HSGS/LOHP.
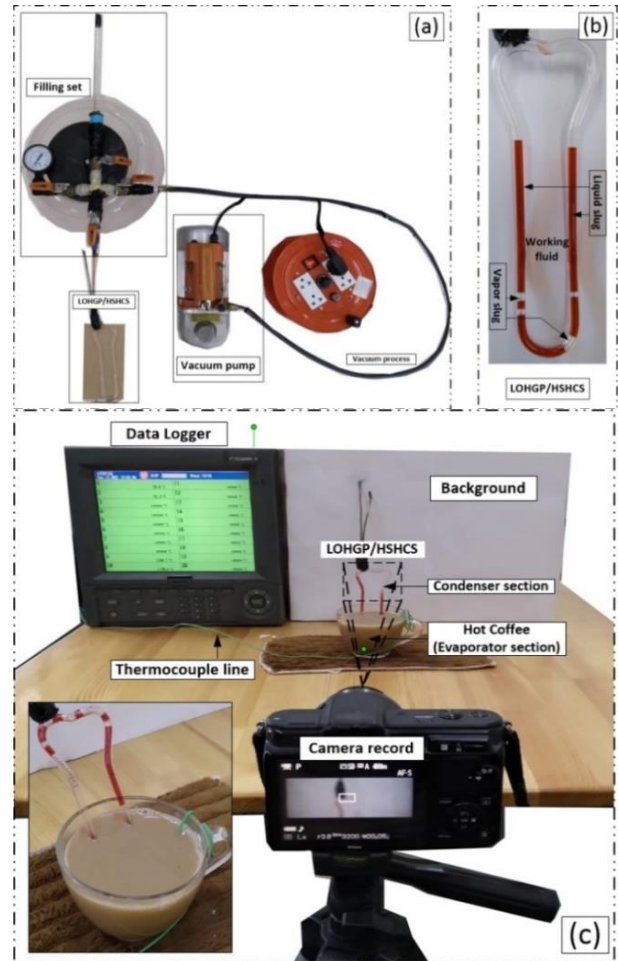

Figure 3. The schematic diagram of the equipment and instrument setup

2.3 Heat transfer rate and flow patterns analysis

The heat transfer rate resulting from the heat conduction from the heat source at the evaporator section through the tube wall is determined by the Fourier equation of thermal conductivity as shown in Eq. (2) [16]:

$$Q_{cond} = kA_e \frac{\Delta T}{t} \tag{2}$$

where, Q_{cond} is the heat transfer rate due to the heat conduction through the pipe wall (W), k is the pipe thermal conductivity (W/m °C), A_e is the evaporator surface area (m²), ΔT is the temperature difference between the outer and inner tube surfaces (°C), and t is the pipe thickness (m).

The heat transfer rate of the two – phase flow pattern at condenser section was determined by natural convection at condenser section which was calculated from Eq. (3) [17-19]:

$$Q = Q_{conv,c} = h_{conv} A_c \left(T_{wall,c} - T_{air} \right) \tag{3}$$

The heat flux or the heat transfer rate/surface area of the condenser (kW/m²) was obtained from the below Eq. (4) [20, 21]:

$$q = \frac{Q}{A_c} \tag{4}$$

where, Q is heat transfer rate (W), h_{conv} is convection heat transfer coefficient (W/m²·°C), A_c is the condenser surface area (m²), $T_{wall,c}$ is the wall temperature of condenser section (°C), T_{air} is air temperature (°C), q is heat flux (kW/m²).

Furthermore, flow behaviors within the tube can be determined by a group of non-dimensional variants or Reynolds Number (Re) as shown in the following Eq. (5) [22]:

$$\mathrm{Re} = \frac{\rho V D}{\mu} = \frac{V D}{\nu} \tag{5}$$

where, V is average flow pattern velocity (m/s), D refers to diameter of flow pattern (m), ρ is density (kg/m³), μ is dynamic viscosity (kg/m·s), and ν is kinematic viscosity (m²/s).

The flow patterns can be divided according to the phase of the working substance inside the heat pipe as follows: liquid phase and gas phase. The working substance inside the heat pipe flows in two – phase, alternating between liquid and gas phase. When the evaporator section is heated, the working substance changes from liquid to gas and moves from the evaporator section through the adiabatic section to the condenser section. This study focused on the flow patterns in the heart-shape area, which served as the condenser section for HSGS/LOHP. The two-phase flow patterns in the condenser section of HSGS/LOHP can be calculated by the buoyancy force equation as shown in the Eq. (6) [23]:

$$F_B = \vee(\rho_l - \rho_v)g \tag{6}$$

where, F_B is the buoyancy force (N), $\vee$ is the volume of the flow pattern (m³), ρ_l, ρ_v is is the density of the liquid phase – vapor phase working substance (Kg/m³), and g is the acceleration due to the gravity (m/s²).
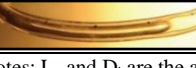
The resistance to the displacement of the flow pattern in the condenser section can be explained by the principle of moment of inertia as shown in Eq. (7):

$$I = \frac{1}{2}mR^2 \tag{7}$$

where, I is the moment of inertia (kg·m²), m is the mass of the flow pattern (kg), and R is the radius of the flow pattern (m).

As per the two - phase flow pattern at the condenser section of HSGS/LOHP, the grouping and classification of the flow patterns was done according to the length of the vapor bubbles along with the photographic observations as shown in Table 2 [12, 24].

Table 2. Grouping and categorization of the flow patterns

Flow patterns	Size	Characteristic and forms
Bubble flow, BF	$L_g < 1.3D_i$	Occurs when the working substance in liquid phase changes to vapor phase. Small bubbles grow larger and appear as spherical vapor bubbles.
Slug flow, SF	$1.3D_i < L_g < 7.5D_i$	Slug flow is formed by merging bubbles from flow patterns or elongation of the bubble. The vapor phase of the working substance takes an elongated oval shape or a bullet shape when moving at high speed. There are brief sections of liquid working substance between the vapor slugs.
Annular Flow, AF	$L_g > 7.5D_i$	Annular flow is formed by merging or elongation of the slug flow. Liquid phase working substance forms a thin film along the pipe wall. The thickness of the film is usually greater at the bottom than the top. The vapor phase working substance appears in the middle of the tube.

Notes: L_g and D_i are the average length of the vapor bubble and the diameter inside the heat pipe, respectively [12, 24].

3. RESULTS AND DISCUSSIONS

As per the application HSGS/LOHP to add uniqueness and attractiveness to a glass spoon, the results of the two - phase flow pattern observation in the heart-shaped part of the spoon indicated that this creation is clearly distinct from the currently used utensils. The results are presented in the following aspects:

3.1 Behaviors and flow patterns at the HSGS/LOHP's condenser

When the HSGS/LOHP's evaporator section (heart-shaped glass spoon) made contact with the heat source (hot coffee in the cup), the heat was transferred through the tube wall by heat conduction to the working substance [22]. When it was heated enough, the working substance in its liquid phase evaporated and resulted in the initial bubble flow patterns. Then, the accumulated energy gathered during its motion changed the flow pattern from bubble flow to slug flow and to annular flow.

As a result, the vapor bubbles in the evaporator section enlarged and the vapor pressure also increased. Therefore, the pressure of the slug flow working substance and the vapor bubbles flowed to the condenser section that had a lower temperature (the heat sink). This force is called the driving force of the oscillating heat pipe which was found in slug flow and annular flow that flowed from the evaporator section to the condenser section of the HSGS/LOHP. This occurred along with the convection heat transfer rate of the two - phase flow pattern from the evaporator section to the condenser section as shown in Figure 4(a)-4(b). Furthermore, the pressure difference between these two parts also increased as the HSGS/LOHP was made from a single coiled capillary tube that made up the evaporator and the condenser sections. This was due to the movement of liquid and vapor bubbles from the evaporator section to the condenser section which led to further movements of liquid and vapor bubbles through the arc to the evaporator section. Thus, a repeated cyclical evaporation of the working substance was observed. When the vapor pressure rose, it produced a restoring force which

pushed the working substance back to the condensation unit again. As a result of this simultaneous thrust between the driving and restoring forces, an oscillating motion of the working substance along the pipe axis was generated [22].
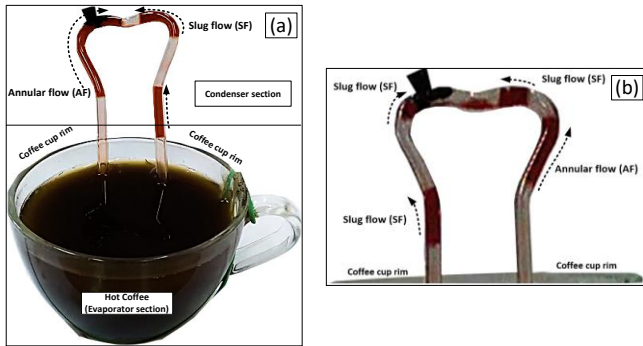

Figure 4. The behavior and flow patterns within the HSGS/LOHP's condenser section

3.2 Effect of filling ratio and evaporator's temperature on the flow pattern within the HSGS/LOHP's condenser section

The nature of the flow patterns within the condenser section of HSGS/LOHP as influenced by the filling rate and the evaporator temperature is shown in Table 3. Two phase flow patterns were observed in the condenser of the HSGS/LOHP, these were slug flow (SF) and annular flow (AF) at the working substance filling rate of 80% and 60%, respectively. For the filling rate of 40%, only slug flow (SF) was found. The increase in the evaporator temperature in all test cases and the different filling ratios resulted in an increase in the velocity of the flow pattern in the condenser section. Higher evaporation temperature allowed the liquid working substance at the evaporator of the HSGS/LOHP to easily boil. The required time to vaporize the liquid working substance was also shortened [24]. Due to the flow patterns change accompanied by the increase in the velocity and pressure of the movement from the vapor, slug and annular bubbles appeared at the condenser section. These are also known as slug and annular flow patterns. Moreover, it was also found that the SF had a higher flow speed than that of the AF due to SF's smaller vapor bubble size and the shape of the HSGS/LOHP condenser which was designed as a heart shape. As the smaller bubbles moved through the bends, they had a faster flow speed than the

bigger ones which corresponds to the explanations in Section 3.3. As per the buoyancy force and moment of inertia of the flow pattern at the condenser, the test data in Table 3 indicated that at the evaporator temperature of 70°C, the flow pattern in all test cases had the highest moving speed. At 40% of the working substance filling rate, an average speed of SF was 0.00171 m/s, which was the highest speed obtained from this test. At this filling rate, a relatively small amount of working substance was added which accelerated the boiling and evaporation of the substance. Hence, the bubbles and vapor could occur more rapidly. This increase in velocity shortened the expansion time of the vapor bubbles in the evaporator, resulting in a smaller average vapor bubble size [24]. Therefore, this was only found in slug flow which had the shortest length in all test cases or 0.0102 m for 40% of working substance filling rate and the evaporator section temperature of 70 °C. This resulted in less volume of the liquid bar and vapor bubbles moving from the evaporator section to the condenser section. This circumstance caused less movement of the liquid bar and the vapor bubble on the other side to pass through the arc to the evaporator section as well. Low vapor pressure and restoring force led to less pressure difference between the evaporator section and condenser section. As such, at 40% working substance filling rate, only the slug flow was observed in the condenser whereas at 60% and 80% working substance filling rates, slug flow and annular flow were observed.

3.3 Effects of the evaporator section temperature on buoyancy and moment of inertia of the flow pattern within the condenser of HSGS/LOHP

Figure 5(a)-5(b) show the relationship of the evaporator temperature and the working substance filling rate effect on the buoyancy force and moment of inertia of the slug and annular flows at the HSGS/LOHP's condenser. According to the data, increased evaporator's temperature resulted in lower buoyancy force and moment of inertia for both the slug (SF) and annular (AF) flow patterns within the HSGS/LOHP's condenser, as shown in Figure 5(a)-5(b), respectively. Due to higher evaporation temperature, the working substance boiled easily and the expansion of the vapor bubbles occurred rapidly. Thus, the bubble's expansion time at the evaporator was reduced [24]. Therefore, the evaporator temperature increase resulted in a shorter length of the flow pattern as shown in Table 3.
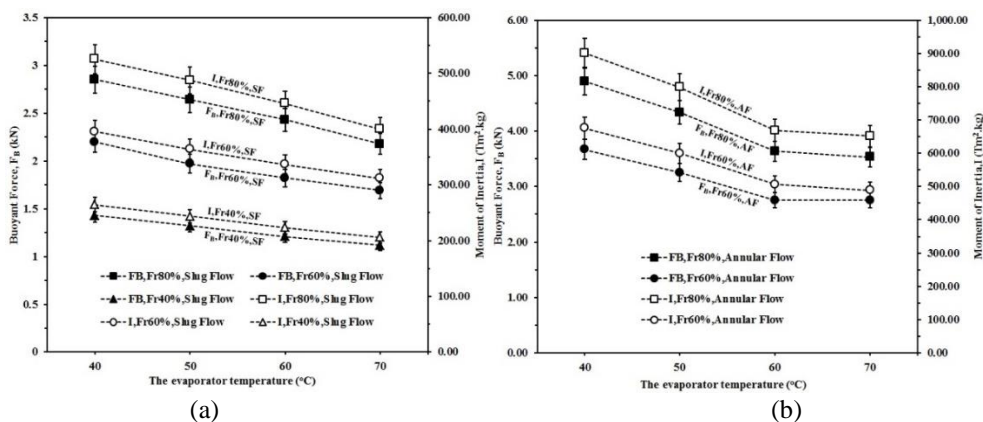

Figure 5. The relationship of the evaporator temperature and the working substance filling rate effect on the buoyancy force and moment of inertia of the slug flow (a) and annular flow (b) in the condenser of HSGS/LOHP

Table 3. The flow patterns within the HSGS/LOHP's condenser as a result of the working substance filling rate and the evaporator's temperature (℃)

The working substance filling rate of 80% of the evaporator section's volume and the temperature at the evaporator (℃).							
70		60		50		40	
V_g (m/s)	L_g (m)	V_g (m/s)	L_g (m)	V_g (m/s)	L_g (m)	V_g (m/s)	L_g (m)
SF=0.00153	SF=0.0197	SF=0.00147	SF=0.0221	SF=0.00116	SF=0.0239	SF=0.00085	SF=0.0259
AF=0.00103	AF=0.0320	AF=0.00091	AF=0.0333	AF=0.00080	AF=0.0393	AF=0.00069	AF=0.0044
The working substance filling rate of 60% of the evaporator section's volume and the temperature at the evaporator (℃).							
70		60		50		40	
V_g (m/s)	L_g (m)	V_g (m/s)	L_g (m)	V_g (m/s)	L_g (m)	V_g (m/s)	L_g (m)
SF=0.00166	SF=0.0153	SF=0.00158	SF=0.0166	SF=0.00123	SF=0.0179	SF=0.00092	SF=0.01943
AF=0.00111	AF=0.0240	AF=0.00099	AF=0.0250	AF=0.00087	AF=0.0295	AF=0.00075	AF=0.0332
The working substance filling rate of 40% of the evaporator section's volume and the temperature at the evaporator (℃).							
70		60		50		40	
V_g (m/s)	L_g (m)	V_g (m/s)	L_g (m)	V_g (m/s)	L_g (m)	V_g (m/s)	L_g (m)
SF=0.00171	SF=0.0102	SF=0.00163	SF=0.0111	SF=0.00126	SF=0.0120	SF=0.00095	SF=0.0130

Notes: V_g, L_g are the velocity and length of the vapor bubbles, respectively.

The reduction of the flow pattern led to a low mass and volume requiring a lower buoyancy or buoyancy force (F_B) for the bubble to flow up to the HSGS/LOHP's condenser. The flow pattern expressed in terms of the lower moment of inertia (I) for the slug and the annular flows is shown in Figure 5(a) - 5(b). This is also explained by the high velocity of the flow pattern when the temperature of the evaporator was increased in both flow patterns at every rate of the working substance filling rate as shown in Table 3. In addition, at the evaporator temperature of 40℃ and 80% working substance filling rate, the annular flow had maximum buoyancy force and moment of inertia of 4.90 ± 0.25 kN and 901.77 ± 45.08 Tm².kg, respectively, as shown in Figure 5(b). At 40% of the working substance filling rate and 70℃ evaporator temperature, the slug flow had the lowest buoyancy force and moment of inertia of 1.12 ± 0.05 kN and 205.77 ±. 10.28 Tm².kg, respectively, as shown in Figure 5(a). At the evaporator temperature of 40℃, accumulation of heat energy within the evaporator took a longer time than that of the 50, 60, and 70℃ which gave the vapor bubbles a longer period of time to expand at the evaporator [24]. As a result, at the evaporator temperature 40℃, the length of the flow pattern for both the slug flow and the annular flow was longer than the evaporator temperature of 50, 60, and 70℃ as shown in Table 3. This eventually

resulted in high values of buoyancy force and moment of inertia at the evaporator temperature of 40℃.

3.4 Effects of the evaporator temperature on Reynolds Number (Re) and Heat Flux in the condenser section of HSGS/LOHP

The increased evaporator temperature helped the working substance in the HSGS/LOHP to be more conducive to boiling at any active substance addition rate. The heat from the heat source permeated through the pipe wall into the working substance within the evaporator which led to its vaporization. This condition initiated the two-phase flow of the working substance from the evaporator to the condenser of the HSGS/LOHP. Increased temperature in Slug flow and Annular flow resulted in lower density, dynamic viscosity and kinematic viscosity of the working substance. As a result, flow pattern movement speed became faster in accordance with the higher evaporator temperature as shown in Table 3.

Upon considering the two-state flow pattern, the Reynolds Number, and the heat flux as shown in Figure 6, test results revealed that the increased temperature also raised value of the Reynolds Number (Re) and the heat flux of the condenser. At HSGS/LOHP's working substance filling rate of 80% of the

evaporation volume, and the evaporative temperature of 70°C, maximum heat flux of 0.01171 kW/m^2 and the Reynolds Number of 8.704 were achieved. Reynolds Number (Re) is a dimensionless variable which is expressed by flow behavior of the fluid within a pipe. The number is relative to properties of the working substance such as density, dynamic viscosity, kinematic viscosity, average velocity of flow in the pipe, pipe diameter, and structural characteristics of the pipe. These properties are influenced by or subjected to the evaporator temperature. The two-state flow pattern carries heat from the evaporator to the condenser [21, 23, 24] as illustrated in the Slug flow and Annular flow of HSGS/LOHP.
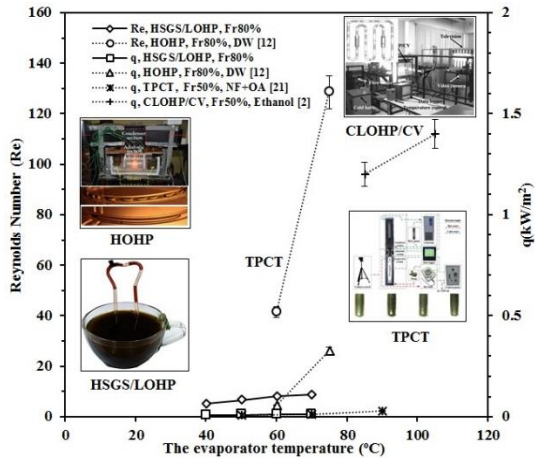

Figure 6. The relationship of the evaporator temperature on Reynolds Number (Re) and Heat Flux in the condenser section of HSGS/LOHP

In addition, previous laboratory scale studies on the two-phase flow patterns of Helical Oscillating Heat Pipe (HOHP) heat exchangers [12], Closed- Loop Oscillating Heat- Pipe with Check Valves (CLOHP/ CV) [2] and Two-Phase Closed Thermosyphon (TPCT) [21] revealed the same trend and direction as those obtained from the HSGS/LOHP. These trend and direction including the heat flux and the Reynolds Number (Re) which increased according to the evaporator temperature as shown in Figure 6.

4. CONCLUSION

This article explored the application of the Heart Shaped Glass Spoon Loop Oscillating Heat Pipe (HSGS/LOHP) which was designed to resemble a coffee spoon in structure and dimensions. HSGS/LOHP can be practically used like the actual coffee spoon. The heart-shaped condensing part of the glass displays the behavior of the two-state flow patterns. The purpose of this research is to provide basic information on the application of Oscillating Heat Pipe (OHP) as a daily used product. The results are summarized as follows:

The heart-shaped glass spoon with oscillating heat pipe can be practically used for which the behavior of slug and annular flow of the working substance within the condenser section can be observed. It is a product design and application that really meets the needs which can be further developed commercially to increase the market value in the coffee industry. The spoon can enhance the product's uniqueness for coffee admirers.

Working substance filling ratio and evaporator temperature

are important for the formation of flow patterns within the condensing unit of HSGS/LOHP. At 60% and 80% of working substance filling rate, 2 flow patterns, slug flow and annular flow were observed within the condenser section of the HSGS/LOHP. This was different from the 40% filling ratio which only exhibited the slug flow. The average length of the flow in each pattern was directly proportional to the working substance filling rate, along with the increase in the average velocity of the flow patterns when the evaporator temperature was increased.

Increased evaporator temperature reduced the buoyancy force and moment of inertia of each flow pattern within the condenser section of HSGS/LOHP. At 40°C, the highest buoyancy force and moment of inertia in each flow pattern for every working filling rate were observed. The lowest buoyancy force and moment of inertia in each flow pattern were found at the evaporator temperature of 70°C.

Increased evaporator temperature raised the Reynolds Number (Re) and the heat flux as the temperature caused the properties of the working substance including density, dynamic viscosity and kinematic viscosity to be lower. As a consequent, flow speed was increased which also resulted in higher heat flux values.

Limitations and problems of this study were mainly due to the production of a coffee stirrer from a glass tube which has similar size and shape to the common coffee spoon. Furthermore, the prototype Heart Shaped Glass Spoon Loop Oscillating Heat Pipe (HSGS/LOHP) was made from a glass tube with a small inner diameter which must be carefully used. Future research may use rigid plastic pipes which may result in a more durable spoon that can be molded into different shapes. This will enhance a better appearance, and further increase its commercial values. Thus, the product can be sold during special events or as souvenir.

REFERENCES

[1] Sanhawat, T. (2010). Factors affecting the flow patterns and heat-transfer characteristics of a top heat mode closed-loop oscillating heat pipe with check valves. Ph.D. Department of Mechanical Engineering, Mahasarakham University, Thailand.

[2] Bhuwakietkumjohn, N., Rittidech, S. (2010). Internal flow patterns on heat transfer characteristics of a closed-loop oscillating heat- pipe with check valves using ethanol and a silver nano - ethanol mixture. Experimental Thermal and Fluid Science, 34(8): 1000-1007.https://doi.org/10.1016/j.expthermflusci.2010.03.003

[3] Rittidech, S. (2010). Heat Pipe Technology. 2 ed. Mahasarakham University.

[4] Supirattanakul, P., Rittidech, S., Bubphachot, B. (2011). Application of a closed-loop oscillating heat pipe with check valves (CLOHP/CV) on performance enhancement in air conditioning system. Energy and Buildings, 43(7): 1531-1535.

https://doi.org/10.1016/j.enbuild.2011.02.017

[5] Rittidech, S., Donmaung, A., Kumsombut, K. (2009). Experimental study of the performance of a circular tube solar collector with closed-loop oscillating heat-pipe with check valve (CLOHP/CV). Renewable Energy, 34(10): 2234-2238. https://doi.org/10.1016/j.renene.2009.03.021

[6] Wannapakhe, S., Chaiwong, T., Dandee, M., Prompakdee, S. (2012). Hot air dryer with closed – loop oscillating heat pipe with check valves for reducing energy in drying process. Procedia Engineering, 32: 77-82. https://doi.org/10.1016/j.proeng.2012.01.1239

[7] Gao, Y., Gao, C., Xian, H., Du, X. (2018). Thermal properties of solar collector comprising oscillating heat pipe in a flat-plate structure and water heating system in low-temperature conditions. Energies, 11(10): 2553. https://doi.org/10.3390/en11102553

[8] Barrak, A.S., Saleh, A.A.M., Naji, Z.H. (2020). An experimental study of using water, methanol, and binary fluids in oscillating heat pipe heat exchanger. Engineering Science and Technology, An International Journal, 23(2): 357-364. https://doi.org/10.1016/j.jestch.2019.05.010

[9] Bhuwakietkumjohn, N., Parametthanuwat, T. (2015). Application of silver nanoparticles contained in ethanol as a working substance in an oscillating heat pipe with a check valve (CLOHP/CV): A thermodynamic behaviour study. Heat and Mass Transfer, 51(9): 1219-1228. https://doi.org/10.1007/s00231-014-1493-z

[10] Liang, C., He, Z., Yang, Y., Zeng, S. (2015). Experimental study on thermal performance of pulsating heat pipe with ethanol-acetone mixtures. International Journal of Heat and Technology, 33(4): 185-190. http://dx.doi.org/10.18280/ijht.330424

[11] Wang, X.H., Jiao, Y.L., Niu, Y.C., Yang, J. (2015). Study on enhanced heat transfer features of nano-magnetic fluid heat pipe under magnetic field. International Journal of Heat and Technology, 33(1): 137-144. https://doi.org/10.18280/ijht.330119

[12] Sriudom, Y., Rittidech, S., Chompookham, T. (2015). The helical oscillating heat pipe: flow pattern behaviour study. Advances in Mechanical Engineering, 7(1): 194374. http://dx.doi.org/10.1155/2014/194374

[13] Krisangsri, P., Hudakorn, T., Sritrakul, N. (2021). Effect of internal diameter and working substances on thermal performance of a vertical closed-loop oscillating heat pipe with double heat sources. Journal of Advanced Research in Fluid Mechanics and Thermal Sciences, 82(2): 120-126.

[14] Satyanand, A., Anand, T., Peter, S., Arvind, P. (2021). Thermal characteristics of a three-dimensional coil type pulsating heat pipe at different heating modes. Thermal Science and Engineering Applications, 13(4): 041011. https://doi.org/10.1115/1.4048760

[15] Rohsenow, W.M. (1952). A method of correlating heat transfer data for surface boiling of liquids. Trans ASME, 74: 969–979. http://hdl.handle.net/1721.1/61431.

[16] JR, M.M.R., Kapuno, R.R.A. (2011). Engineering Heat Transfer. 2 ed. Jones and Bartlett Publishers, LLC.

[17] Thongdaeng, S., Pipatpaiboon, N., Donmuang, A. (2020). Visualization and heat transfer in a closed loop thermosyphon with a check valve. Case Studies in Thermal Engineering, 22: 100758. https://doi.org/10.1016/j.csite.2020.100758

[18] Wannagosit, C., Sakulchangsatjatai, P., Kammuang-lue, N., Terdtoon, P. (2018). Validated mathematical models of a solar water heater system with thermosyphon evacuated tube collectors. Case Studies in Thermal Engineering, 12: 528-536. https://doi.org/10.1016/j.csite.2018.07.005

[19] Nakkaew, S., et al. (2019). Application of the heat pipe to enhance the performance of the vapor compression refrigeration system. Case Studies in Thermal Engineering, 15: 100531. https://doi.org/10.1016/j.csite.2019.100531

[20] Parametthanuwat, T., Pipatpaiboon, N., Bhuwakietkumjohn, N., Sichamnan, S. (2021). Heat transfer characteristics of closed-end thermosyphon (CE-TPCT). Engineering Science and Technology, an International Journal, 27: 101020. https://doi.org/10.1016/j.jestch.2021.05.024

[21] Sichamnan, S., Chompookham, T., Parametthanuwat, T. (2020). A case study on internal flow patterns of the two-phase closed thermosyphon (TPCT). Case Studies in Thermal Engineering, 18: 100586. https://doi.org/10.1016/j.csite.2020.100586

[22] Piyanun, C. (2012). Heat Pipe Technologies. Focus Printing Co., Ltd.

[23] Thongdaeng, S., Rittidech, S., Bubphachot, B. (2012). Flow patterns and heat-transfer characteristics of a top heat mode closed-loop oscillating heat pipe with check valves (THMCLOHP/CV). Journal of Engineering Thermophysics, 21(4): 235-247. https://doi.org/10.1134/S1810232812040029

[24] Sriudom, Y. (2015). Flow patterns and heat transfer characteristics of a helical oscillating heat pipe. Ph.D. Department of Mechanical Engineering, Mahasarakham University, Thailand.

NOMENCLATURE

d	diameter of the capillary tube, m
g	acceleration due to gravity, m/s^2
Q	heat transfer rate, W
k	thermal conductivity, $W/m \cdot {}^\circ C$
A	surface area, m^2
ΔT	temperature difference, ${}^\circ C$
t	thickness, m
h	heat transfer coefficient, $W/m^2 \cdot {}^\circ C$
T	temperature, ${}^\circ C$
q	heat flux, kW/m^2
Re	Reynolds Number
V	average flow pattern velocity, m/s
D	diameter of the flow pattern, m
F	force, (N)
I	moment of inertia, $kg \cdot m^2$
m	mass of the flow pattern, kg
R	radius of the flow pattern, m
BF	Bubble flow
SF	Slug flow
AF	Annular flow

Greek symbols

σ	surface tension, N/m
ρ	density, kg/m^3
μ	dynamic viscosity, $kg/m \cdot s$

ν	kinematic viscosity, m^2/s	v	vapor
∨	volume of flow pattern, m^3	cond	conduction
		e	evaporator
Subscripts		c	condenser
		conv	convection
i	internal	wall	wall
max	maximum	air	air
l	liquid	B	buoyancy